Moving Toward Smart, Resilient and Sustainable Bridges –
Catbas, Frangopol & Yun (Eds)
© 2026 The Author(s), ISBN: 978-1-041-31173-7

Practical implications of recent research on proof load testing

E.O.L. Lantsoght
Universidad San Francisco de Quito, Quito, Ecuador
Delft University of Technology, Delft, The Netherlands
Luleå University of Technology, Luleå, Sweden

R. de Vries
Delft University of Technology, Delft, The Netherlands
TNO, Delft, The Netherlands

G.I. Zarate Garnica
Delft University of Technology, Delft, The Netherlands
Ney and Partners, Delft, The Netherlands

Y. Yang
Delft University of Technology, Delft, The Netherlands

M.A.N. Hendriks
Delft University of Technology, Delft, The Netherlands
NTNU, Trondheim, Norway

ABSTRACT: Proof load testing can be used to directly assess bridges. Over the past six years, fundamental research has been carried out at Delft University of Technology to derive mechanics-based shear stop criteria and to enable structural reliability updating via Bayesian methods. To translate these research findings into recommendations for practice, aspects related to determining the target load, location of the load, location of the sensors, and practical implementation steps have been addressed. This paper illustrates these recommendations with a hypothetical case study showing the influence on the preparation and execution of proof load tests. The result is practical guidance for proof load testing, demonstrating how information sources can be combined to achieve minimal target loads. While application via a full-scale test is pending, these recommendations reflect the latest research insights into proof load testing and its implementation strategies.

1 INTRODUCTION

As many bridges are reaching the end of their originally foreseen service life, assessment of existing bridges becomes increasingly important (Lantsoght 2023, Lantsoght et al. 2024, Cervantes et al. 2025, Bertola et al. in press). One way to improve the assessment of existing bridges is the use of proof load testing (Lantsoght et al. 2022). In a proof load test, it is demonstrated directly that the critical section, span or the superstructure in its entirety fulfils the code requirements regarding structural reliability.

Over the past six years, fundamental research has been carried out at Delft University of Technology to derive mechanics-based shear stop criteria for proof load testing of structures without shear reinforcement (such as reinforced concrete slab bridges) and to enable structural reliability updating via Bayesian methods. The research on shear stop criteria combined analytical and experimental work. The analytical work consisted of deriving mechanics-based shear stop criteria using the Critical Shear Crack Theory and the Critical Shear Displacement Theory

DOI: 10.1201/9781003778677-124

(Zarate Garnica et al. 2024b). The experimental work consisted of two series of experiments on reinforced concrete slabs: one on straight slabs (Zarate Garnica et al. 2024a) and another on skewed slabs (Lu et al. 2025), extended with the data from a series of slab strips carried out earlier (Koekkoek and Yang 2016). This work is translated into a traffic light system, which indicates various levels of warning during a proof load test (Zarate Garnica et al. 2025), including further theoretical work on flexural stop criteria (Lantsoght et al. 2019) as well as the earlier determined stop criteria based on acoustic emissions measurements (Zhang et al. 2025).

The research on structural reliability through Bayesian updating shows how the reliability index changes before, during, and after a proof load test. Four main topics were addressed in this research: time-dependence, measurement data, knowledge level, and spatial uncertainty. The time-dependence was studied by examining changes in the reliability index over time as a function of increasing loads, capacity deterioration, and the effect of one or multiple successful proof load tests (de Vries et al. 2023a). In terms of knowledge level, a lower-bound approach (no information on capacity) can be distinguished from a fully informed case (complete information on capacity). If bridge-specific resistance information is lacking, its capacity may be reverse-engineered from the standards applicable at the time it was originally designed (Harrewijn et al. 2021). Most cases will fall between the lower-bound and the fully-informed case, requiring the specification of a suitable prior distribution for the resistance, which will subsequently be updated with testing information (de Vries et al. 2023b). In the resulting Bayesian framework, various sources of information can be combined with proof load testing outcomes to yield increasingly accurate reliability estimates. In particular, measurements during the proof load test can be used to update the structural reliability index during and after the test through a statistically described indicator, determined analytically, numerically, or derived from previous experiments, for both shear and flexure (de Vries et al. 2025). Ultimately, the effect of spatial variability and system reliability was examined to demonstrate that a reduced number of load tests can demonstrate sufficient reliability of multiple sections, failure modes, and even spans (de Vries et al. in review).

These scientific advances are translated into recommendations for practice, focusing on the aspects related to determining the target load, location of the load, location of the sensors, and practical implementation steps. This paper summarizes the translation of research insights into practical recommendations and shows the application to two hypothetical case studies. Further details of the presented work can be found in the background reports, respectively presenting the practical recommendations of the two research projects (Lantsoght et al. 2025a, Lantsoght et al. 2025b).

2 RECOMMENDATIONS

2.1 *Stop criteria*

Stop criteria are typically used in combination with a fixed target load, which must be reached to demonstrate sufficient reliability. If a bridge has a single governing component (e.g. bending failure at midspan), the ability to withstand the target load directly demonstrates adequate reliability. In this case, stop criteria serve as a damage mitigation strategy that prevents unwanted deterioration resulting from extensive cracking and similar effects. However, if system effects play a role and force redistribution can occur while resisting the target load, verifying each component separately does not demonstrate overall structural safety. In this scenario, stop criteria also help to detect and prevent such force redistribution.

Table 1 gives the traffic light system (developed, validated and detailed in Zarate Garnica et al. 2025) for stop criteria developed by combining theoretical considerations, acoustic emissions-based criteria, and expanding earlier work on flexure. Reaching a green light indicates that the section changes from uncracked to cracked, and relates to overall structural performance and serviceability limit state. The yellow light is an intermediate warning level, whereas a red light indicates that further loading can result in local collapse. The highlighting in Table 1 indicates the associated traffic light color of the criterion. The application of the criteria using AE is detailed in (Zhang et al., 2025). In Table 1, the criterion based on the Critical Shear Displacement Theory is determined by limiting the indicator I_{CSDT} to the limiting value $I_{CSDT,cr}$ which is achieved when the critical shear displacement Δ_{cr} is reached:

$$I_{CSDT,cr} = 0.03|f_c^{0.56}\frac{s_{cr}}{d}\left(-978\Delta_{cr}^2 + 85\Delta_{cr} - 0.27\right) \tag{1}$$

with f_c the cylinder concrete compressive strength, d the effective depth, and the critical shear displacement, which can be multiplied by 1.27 for slabs to account for the waviness of the crack profile in the transverse direction:

$$\Delta_{cr} = \frac{25d}{30610\phi_{eq}} + 0.0022 \leq 0.025 \tag{2}$$

as a function of the equivalent reinforcement diameter φ_{eq}:

$$\phi_{eq} = \frac{\Sigma\phi_i^2}{\Sigma\phi_i} \tag{3}$$

and the height of the fully developed crack s_{cr} is a function of the modular ratio n and the reinforcement ratio ρ:

$$s_{cr} = \left(1 + \rho n - \sqrt{\rho n + (\rho n)^2}\right)d \tag{4}$$

The stop criterion based on the Critical Shear Crack Theory is (Zarate Garnica et al. 2024b):

$$I_{CSCT} = \tau\left(1 + 120\frac{w}{d_g}\right) \leq \frac{\sqrt{f_c}}{3} \tag{5}$$

with τ the shear stress, w the crack width, and d_g the maximum aggregate size.

2.2 *Structural reliability*

To translate the research findings into practical results, two methods are proposed: Level 1 (with two sublevels) and Level 2. Level 1 is a lower-bound approach that operates solely on load effects and does not require information about the capacity. In Level 1a, conservative proof load factors are derived by considering only first-lane 'truck' load effects, and assuming no correlation between traffic and proof load effect model uncertainties. Using this strategy, weigh-in-motion (WIM) data from the Netherlands were used to derive proof load factors for simply-supported bridges (de Vries et al. 2023a). This method is broadly applicable and can be considered easy in its application. As an example, a factor of 1.43 for shear and 1.41 for bending moment applies for a span length of 10 m in CC3, without considering dynamic effects. As a sophistication, Level 1b requires additional preparation and the use of case-specific probabilistic calculations to determine the proof load factor. In Level 2, Bayesian structural reliability updating is performed based on in-situ measurement data and requires more advanced probabilistic calculations but results in accurate reliability predictions (de Vries et al. 2025). This level is primarily of interest when a refined assessment is necessary with as low a proof load as possible, and when the chance of failure during the test is of particular interest because of the societal value of the asset. Evaluating during-test failure probabilities offers an alternative to stop criteria (Section 2.1) suitable for an informed decision-making context. On the other hand, this method can also be cost-efficient for smaller structures that are relatively common, so that the cost of the preparation can be balanced with the more advanced proof load testing application. It should be noted that statically-derived proof load factors need to be multiplied by a factor of 1 to 1.5 to account for dynamic effects, which are a function of the particular bridge configuration (influence length, number of lanes, deck construction, etc.).

When Level 2 is used, the following steps are necessary:

1. Determine the indicator(s) to use during the test, as a function of the expected failure mode(s) during the test.
2. Process the data to determine the relation between the measured value and maximum value of the indicator during the proof load test.
3. Measure the same indicator during the experiment.
4. Use the measurement data as input to determine the reliability index during and after the proof load test for each load step.

Table 1. Traffic light system for stop criteria, indicating both the criteria for beams and slabs.

Objective	Indicator	Physical meaning
Serviceability limit state	$w_{avg} = \frac{\varepsilon_{c,average} l_g}{n_{cr}} \leq 0.3mm$ with n_{cr} the average number of cracks within the gauge length l_g and $\varepsilon_{c,average}$ the average concrete strain	Onset of cracking in reference region
Serviceability limit state	AE-based green-light criterion	Wave-based signal of cracking detected
Shear	min(I_{CSDT}, I_{CSCT}) in section at $0.8 < M/(Vd) \times 1/\lambda < 1$ with $\lambda = a/d$ in beam members	Local reaching of lower bound of shear capacity from mechanical models
Shear	min(I_{CSDT}, I_{CSCT}) near load for loads in middle of width and in section at $0.8 < M/(Vd) \times 1/\lambda < 1$ for loading near edge in slab members	Local reaching of lower bound of shear capacity from mechanical models
Shear	AE-based yellow-light criterion	Cracking in the strut
Shear	AE-derived Damage ratio of 0.5	Half of the strut width deteriorated
Flexure	$w_{res} \leq 0.2 w_{max}$ (w_{res} the residual crack width after load removal, w_{max} the crack width at maximum loading) for members previously cracked in bending $w_{res} \leq 0.3 w_{max}$ for members not previously cracked in bending stiffness reduction, deflection profiles	Changes in flexural behavior and load distribution occurring
Shear	min(I_{CSDT}, I_{CSCT}) in section at $< M/(Vd) \times 1/\lambda < 0.7$ in beam members	Shear-carrying mechanisms nearly achieved in critical region
Shear	min(I_{CSDT}, I_{CSCT}) at $1.5d$ in the middle as well as at $2d$ in width direction from load for loads in middle of width and in section at $M/(Vd) \times 1/\lambda < 0.7$ for loading near edge in slab members	Local reaching of aggregate interlock capacity
Shear	Further development of inclined cracks, typically monitored using DIC	Full shear cracking
Shear	Red-light AE criterion	Cracking in strut significantly reduces capacity
Shear	Damage ratio near 1	Almost entire strut width deteriorated
Flexure	Strain stop criterion: $\varepsilon_c \leq \varepsilon_{c,bot,\max} - \varepsilon_{c0} = \varepsilon_{stop}$ with $\varepsilon_{c,bot,max} = \frac{h-c}{d-c} \times \frac{f_{ym}}{E_s}$ ε_{c0} the analytically determined short-term strain in the concrete caused by the permanent loads, $\varepsilon_{c,bot,max}$ is the concrete strain at that corresponds to a yield stress in the steel, c is the height of the compression zone, h is the height of cross-section, f_{ym} is the average yield strength of the tension reinforcement steel, E_s is the modulus of elasticity of the steel. Crack width stop criterion: $w_{stop} = 2\frac{f_{ym}-f_{perm}}{E_s}\beta_{fr}\sqrt{d_c^2 + \left(\frac{s}{2}\right)^2}$ f_{perm} is the stress in the steel from the permanent loads, β_{fr} is the strain gradient factor used in the method of Frosch (Frosch 1999), d_c is the cover to the centroid of the tension reinforcement, s is the reinforcement spacing.	Local yielding of reinforcement steel

5. The proof load test is finalized when either 1) the calculations from step 4 indicate sufficient reliability after the test, or 2) the test needs to stopped because the reliability index during the test calculated in step 4 has become too low or a stop criterion is reached.

When a subset of n spans out of a total of N spans are tested, transfer factors can be used to multiply the proof load, see Table 2 for the case of flexure. Similar factors have been derived for shear as well (de Vries et al. in review).

Table 2. Transfer factors for multiple simply supported spans of 10 m for flexure.

	n						
N	1	2	3	4	5	6	8
1	1	–	–	–	–	–	–
2	1.13	1	–	–	–	–	–
3	1.17	1.07	1	–	–	–	–
5	1.21	1.11	1.07	1.03	1	–	–
8	1.23	1.14	1.11	1.08	1.05	1.03	1
10	1.25	1.16	1.12	1.09	1.07	1.05	1.02
20	1.28	1.19	1.15	1.13	1.11	1.10	1.07

Moreover, it is possible to cover various sections of the structure with a single position of the applied load in the test. To achieve this, there are two options. The first option is to place the load at a critical position and increase its magnitude until the reliability indices of all relevant cross-sections are high enough. In a two-span bridge example, increasing the proof load factor from 1.45 to 1.55 of the tandem placed at 2.5 m from the support proved sufficient to capture multiple sections and the failure modes of shear and flexure. The second option is to use a vehicle and test all locations by driving the vehicle over the bridge. An example of a short span (10 m) bridge showed that a dump truck with axle loads of 40 tons spaced at 1.3 m and a distance of 6 m between the trucks, or a trailer with eight axles of 25 tons spaced at 1.5 m would be suitable vehicles to demonstrate a sufficiently large reliability index.

3 CASE STUDIES

3.1 *Case study 1*

The first case study highlights the measurement locations and selected instrumentation for a fictitious case study viaduct of four spans, with end spans of 10 m and middle spans of 15 m in which a proof load test for shear is carried out (placing the tandems at 2.5 m) in the first span. A skew angle of 20 degrees is considered and the width is 6.6 m. The concrete compressive strength can be assumed as 45 MPa. This fictitious case study is a simplification of viaduct Zijlweg (Lantsoght et al. 2017) and a proof load tandem of 1250 kN is applied in the obtuse corner at 1.8 m from the edge of the slab. The goal of this case study is to find the location to apply the sensors, by finding the regions with $0.8 < M/(Vd) \times 1/\lambda < 1$ for the yellow light and $M/(Vd) \times 1/\lambda < 0.7$ for the red light criterion. To find these locations, a linear finite element model is made in Scia Engineer 22.1 (Nemetschek Scia 2022), see Figure 1. For the applied load, the plots of m_x and v_x are derived. These values are exported, and a plot of $M/(Vd) \times 1/\lambda$, shown on a straight grid to facilitate the calculations, is then determined, see Figure 2. From Figure 2, it can be seen that for a skewed slab member, with the load close to the edge and in the obtuse corner, the identification of the critical locations is not as straightforward as for a straight slab with the load in the middle.

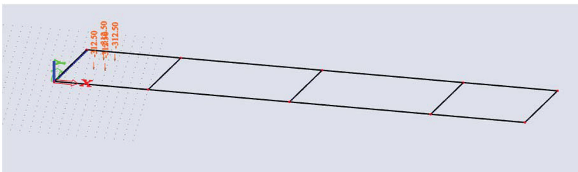

Figure 1. Scia model of case study slab bridge.

Based on the current recommendations, the minimum number of sensors (linear variable displacement transducers, LVDTs) to measure deformations is three, and they should be placed as follows:

- In the yellow light region $0.8 < M/(Vd) \times 1/\lambda < 1$: LVDT1 in the middle of the front axle of the tandem.

- In the red light region $M/(Vd) \times 1/\lambda < 0.7$. It is proposed to place an LVDT at $x = 2.5$ m and $y = 5.5$ m (LVDT2, at the height of the first axle of the tandem but closer to the free edge) and in the region with $x = 1.5$ m and $y = 4$ m (LVDT3, between the first axle and the nearest support).

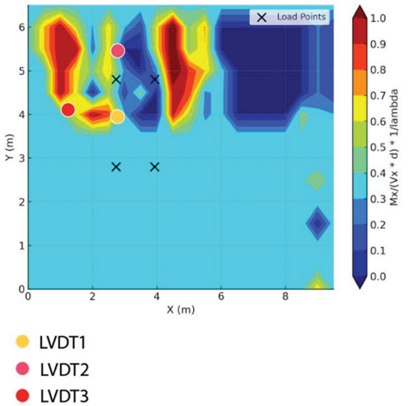

Figure 2. Calculated values of $M/(Vd) \times 1/\lambda$, shown on a straight grid, showing also location of the loading points and location of the instrumentation.

In addition, it is recommended to use DIC in the region of the applied load and the support to follow the development of cracks during the test. To complete the measurement plan, the following sensors should also be added:

- load cells at the locations of the four applied loading points to measure the applied load;
- LVDT4 near LVDT1 to measure the opening of n existing crack, or in the middle of the tandem, to check w_{avg};
- acoustic emission measurements to follow the stop criteria for shear and flexure based on acoustic emissions;
- LVDT5 for the deflection in the center of the tandem to determine the load-displacement diagram;
- LVDT6 to measure the deflection at the supports for correction;
- Three additional deflections in the longitudinal direction (LVDTs 7-9) and transverse direction (LVDTs 10-12) to develop the deflection profiles;
- LVDT13 to measure strains caused by changes in temperature and humidity.

3.2 *Case study 2*

To apply the recommendations based on the structural reliability research, a simply supported case study is considered. A simply supported slab of 10 m with one traffic lane, and all dimensions similar to the previous case study, is used for this application. To apply Level 1, for a proof load test considering shear, the axles load for a LM1-tandem that corresponds to the load effect of the Eurocode load, multiplied by 1.43 is sought. In addition, a dynamic amplification factor of 1.1 is taken into consideration. First, a distributed load of 9 kN/m^2 and two axles of 300 kN are applied to the Scia model, without load factors, see Figure 3. The resulting shear stress, averaged over 4d, is 33.54 kN/m, see Figure 4. Applying only the tandem results in a shear stress of 25.90 kN.m. The required proof load is thus:

$$300\text{kN}\frac{33.54\,\frac{\text{kN}}{\text{m}}}{25.90\,\frac{\text{kN}}{\text{m}}} \times 1.43 \times 1.1 = 611.1\,\text{kN per axle}$$

or 305.6 kN per wheel. This value is slightly smaller than the value of 312.5 kN that was used based on the reference of the Zijlweg viaduct case study. A relatively low value of the dynamic amplification factor of 1.1 is used here, because it is assumed that this particular bridge is effective at damping vibrations caused by traffic. Additional case studies have been developed, including a four-span reinforced concrete slab bridge case (de Vries et al. 2025) as well as a theoretical case of two spans (de Vries et al. in review).

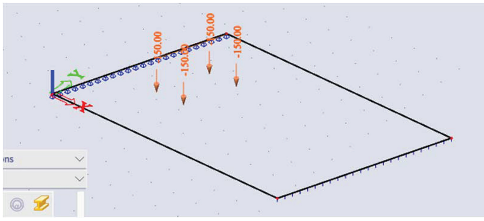

Figure 3. Simply supported slab model, showing tandem with two axles of 300 kN.

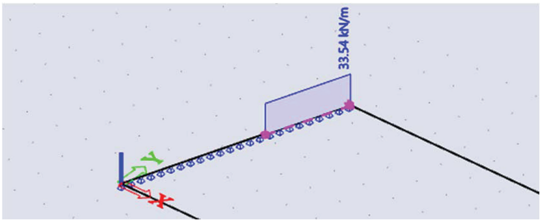

Figure 4. Resulting averaged shear.

4 SUMMARY AND CONCLUSIONS

This paper describes the translation of the research insights into practical recommendations, illustrated with two hypothetical case studies showing the influence of these new recommendations on the preparation and execution of proof load tests. Based on the presented results, the following conclusions can be drawn:

- A traffic light system for stop criteria for non-shear-reinforced members combines serviceability limit state, and the ultimate limit state failure modes of flexure and shear. Using a traffic light system is an innovative way to add more meaning to the measurements obtained during the test.
- The probabilistic studies have resulted in a Bayesian framework where various blocks can be implemented to extract value from various sources of information, particularly measurements during proof load testing. A lower-bound method with a proof load factor and transfer factors is available, although in many cases applying the Bayesian framework will result in bridge-specific, typically lower, test loads and indicate the failure probability during the test.
- The two case studies are used to demonstrate the translation of the recommendations into practical applications, including the development of a measurement plan for the first case study and determining the tandem axle load corresponding to the Level 1a lower-bound load-effect for the second case study.

The result of this work is practical guidance for proof load testing, demonstrating how past research into stop criteria and structural reliability is applied in two case studies. These recommendations reflect the latest research insights into proof load testing and its implementation strategies.

Further work consists in the verification with a full-scale test to verify applicability and practical application. Ideally, the field test should combine a proof load test and collapse test to determine the margin of safety.

ACKNOWLEDGMENTS

The authors would like to acknowledge Rijkswaterstaat for funding this research, and thank Sonja Fennis and Marius Naaktgeboren for the fruitful discussions.

REFERENCES

Bertola, N., Bhowmick, A., Casas, J. R., Chacon, R., Cousins, D., Grimson, J., Lantsoght, E. O. L., Losanno, D., Olaszek, P., Sas, G., Schmidt, J. W., Valenzuela, M. A. & Žnidarič, A. in press. Bridge Load Testing for Assessment: Recent Advances in Application, Collaboration, Codes, and Research. *Structure and Infrastructure Engineering*. https://doi.org/10.1080/15732479.2025.2594077

Cervantes, E., Castellanos, L., Matos, J. C. & Lantsoght, E. Condition assessment of reinforced and prestressed concrete bridges using visual inspection and 3D modeling. I*ABSE Congress Ghent 2025: The Essence of Structural Engineering for Society*, 2025. International Association for Bridge and Structural Engineering (IABSE), 553–562.

De Vries, R., Lantsoght, E. O., Steenbergen, R. D. & Naaktgeboren, M. 2023a. Proof load testing method by the American association of state highway and transportation officials and suggestions for improvement. *Transportation research record*, 2677, 245–257.

De Vries, R., Lantsoght, E. O. L., Steenbergen, R. D. J. M. & Fennis, S. A. A. M. 2023b. Time-dependent reliability assessment of existing concrete bridges with varying knowledge levels by proof load testing. *Structure and Infrastructure Engineering*, 1–15.

De Vries, R., Lantsoght, E. O. L., Steenbergen, R. D. J. M., Hendriks, M. A. N. & Fennis, S. A. A. M. in review. Addressing spatial correlation and system reliability in proof load testing of reinforced concrete bridges and viaducts. *Structural Safety*.

De Vries, R., Lantsoght, E. O. L., Steenbergen, R. D. J. M., Hendriks, M. A. N. & Naaktgeboren, M. 2025. Structural reliability Updating on the basis of proof load testing and monitoring data. *Engineering Structures*, 330, 119863.

Frosch, R. J. 1999. Another Look at Cracking and Crack Control in Reinforced Concrete. *ACI Structural Journal*, 96.

Harrewijn, T., Vergoossen, R. & Lantsoght, E. Reverse engineering of existing reinforced concrete slab bridges. IABSE Congress, Christchurch 2021: Resilient technologies for sustainable infrastructure, 2021.

Koekkoek, R. T. & Yang, Y. 2016. Measurement Report on the transition between flexural and shear failure of RC beams without shear reinforcement. Delft University of Technology.

Lantsoght, E., Yang, Y. & Hendriks, M. Extending the service life of existing concrete bridges using improved assessment methods. IABSE Congress 2024: Beyond Structural Engineering in a Changing World, 2024. IABSE, 227–234.

Lantsoght, E., Zarate Garnica, G. I., Yang, Y. & Hendriks, M. A. N. 2025a. Proefbelasten van dwarskrachtkritische betonnen plaatviaducten. Stevin Report 25.5 25–01. Delft University of Technology.

Lantsoght, E. O. 2023. Assessment of existing concrete bridges by load testing: barriers to code implementation and proposed solutions. *Structure and Infrastructure Engineering*, 1–13.

Lantsoght, E. O. L., De Vries, R., Yang, Y. & Hendriks, M. A. N. 2025b. Probabilistische onderbouwing proefbelasten: praktische inzichten. Delft University of Technology. Stevin Report 25.5 25-03. Delft University of Technology.

Lantsoght, E. O. L., Koekkoek, R. T., Hordijk, D. A. & De Boer, A. 2017. Towards standardization of proof load testing: pilot test on viaduct Zijlweg. *Structure and Infrastructure Engineering*, 16.

Lantsoght, E. O. L., Yang, Y. & Van Der Veen, C. 2022. Multi-level decision-making strategy for preparation of proof load and failure tests. *Engineering Structures*, 252, 113672.

Lantsoght, E. O. L., Yang, Y., Van Der Veen, C., Hordijk, D. A. & De Boer, A. 2019. Stop Criteria for Flexure for Proof Load Testing of Reinforced Concrete Structures. *Frontiers in Built Environment*, 5.

Lu, J., Yang, Y., Hendriks, M. A. N. & Lantsoght, E. O. L. 2025. Experiments on skewed reinforced concrete slabs failing in shear. *IABSE Congress Ghent 2025 – The Essence of Structural Engineering for Society*. Ghent, Belgium.

Nemetschek SCIA 2022. Scia helpfile release 22.1.3016.64.

Zarate Garnica, G., Lu, J., Yang, Y., Hendriks, M. A. N. & Lantsoght, E. O. L. 2024a. Shear Experiments On Straight Reinforced Concrete Slabs. *Proceedings of International Structural Engineering and Construction: March*, 11, 1.

Zarate Garnica, G. I., Lantsoght, E. O. L., Yang, Y. & Hendriks, M. A. N. 2024b. Shear stop criteria for reinforced concrete slab strips. *IABMAS 2024*.

Zarate Garnica, G. I., Zhang, F., Yang, Y., Hendriks, M. A. N. & Lantsoght, E. O. L. 2025. Stop criteria for proof load testing using a traffic light system. *IABSE Congress Ghent 2025 – The Essence of Structural Engineering for Society*. Ghent, Belgium.

Zhang, F., Yang, Y. & Hendriks, M. A. N. 2025. Acoustic emission-based indicators of shear failure of reinforced concrete beams without shear reinforcement. *Engineering Structures*, 330, 119929.